MJFAS MALAYSIAN JOURNAL OF FUNDAMENTAL AND APPLIED SCIENCES
PRINT ISSN: 2289-5981 | ONLINE ISSN: 2289-599X

RESEARCH ARTICLE

Thermoluminescence studies of calcium metaborate (CaB_2O_4) nanocrystals synthesized by solution combustion method

T. N. H. Tengku Kamarul Bahri *, R. Hussin, N. E. Ahmad

Department of Physics, Faculty of Science, Universiti Teknologi Malaysia, 81310 UTM Johor Bahru, Johor, Malaysia

* *Corresponding author: tnhidayah2@gmail.com*

Article history
Received 18 February 2017
Accepted 6 December 2017

Abstract

This paper presents the thermoluminescence properties of calcium metaborate (CaB_2O_4) nanocrystals prepared by solution combustion method. The samples were characterized by X-ray diffraction (XRD), field emission scanning electron microscopy (FESEM), energy dispersive X-ray (EDX) and thermoluminescence (TL) analysis respectively. The XRD patterns showed the orthorhombic structure with the crystallite size at around 27 nm and the FESEM micrograph revealed the formation of nanocrystals with irregular spherical shape. Weight fraction obtained from EDX analysis consequently led to determination of an effective atomic number. It was found that the effective atomic number of CaB_2O_4, Z_{eff} = 14.1 was equivalent to the effective atomic number of the bone, Z_{eff} = 13.2 with error of 6.8 %. The samples were annealed using the TLD oven and exposed to Cobalt-60 source. TL glow curves were recorded using a Harshaw model 3500 TLD reader. The TL glow curve of this material showed a simple, single, peak located at around 150 °C. The most striking dosimetric feature of these nanocrystals was the excellence of the linearity response of a dose range from 1 Gy up to 100 Gy with R^2= 0.9827 compared to the TLD-100 powder with R^2= 0.9276. The high linear correlation between dose and TL response to gamma radiation suggests that calcium metaborate nanocrystals can be considered as a promising material to be used in thermoluminescence dosimetry.

Keywords: Calcium borate, nanocrystals, thermoluminescence, solution combustion, dosimetric

INTRODUCTION

The physical process of thermal release of stored, radiation induced luminescence, known as thermoluminescence (TL), was used for the detection of ionizing radiation (Wiedemann and Shmidt, 1895). Solid state dosimetry (which is the integrating measurement of directly or indirectly ionizing radiation by means of radiation) induced changes in inorganic and organic crystals and glasses have received serious attention. A lithium fluoride that is activated with magnesium and titanium (LiF: Mg, Ti) (called TLD-100) is the most widely-used TL phosphor and the best-known solid state dosimetry. However, with the rapidly increasing use of radiation sources, it is realized that the capabilities of thermoluminescence in such materials as LiF: Mg, Ti (TLD-100) as a large scale, long-term dosimeter are rather limited. The main reasons include: its being hygroscopic; having an expensive TL phosphor; being applicable to a limited dose range; and having the need for a rather complex annealing processing procedure. Hence, an intense search for alternative, sufficiently stable, and sensitive physical effects in solids have been produced until now.

Calcium metaborate (CaB_2O_4) is one of the most widely-studied oxide materials because it presents good chemical stability due to low hygroscopic nature (Santiago et al., 2001) and a linear response in X-ray dose range 1 to 10000 mGy for polycrystalline CaB_2O_4 (Fujimoto et al., 2015). Also, CaB_2O_4 showed a simple annealing procedure as reported earlier (Tengku Kamarul Bahri et al., 2017). The solution combustion method, which is known to prepare nanophosphors, has been regarded as one of the more effective and economic methods due to its convenient processing, significant time-saving attributes and simple experimental setup compared to the phosphor obtained via other conventional solid-state methods. Therefore, the present work deals with nanocrystalline CaB_2O_4 powder, prepared by solution combustion method. The aim of this study is to determine the thermoluminescence properties of CaB_2O_4 nanocrystals that are required for thermoluminescence dosimetry (TLD) of gamma ray of Cobalt-60. Specifically, glow curve, dose response, TL sensitivity and effective atomic number are studied. For comparison, glow curves are recorded for TLD-100. The X-ray diffraction (XRD) spectroscopy, field emission scanning electron microscopy (FESEM), and energy dispersive X-ray (EDX)characterizations of the sample are also presented here.

EXPERIMENTAL

Materials

The starting raw materials used include analytical pure grade calcium nitrate; tetrahydrate; ($Ca(NO_3)_2.4H_2O$, 99 %, Merck KGaA, Germany); boric acid (H_3BO_3, 99.5 %, Merck KGaA, Germany); urea (CH_4N_2O, 98 %, Sigma – Aldrich, Missouri) and ammonium nitrate (NH_4NO_3, 95 %, Merck KGaA, Germany) respectively.

Synthesis of CaB_2O_4 powder

Fig. 1 shows the preparation of CaB_2O_4 powder by solution combustion method. The raw materials were weighed according to the chemical composition of CaB_2O_4 and put in a 100 ml beaker. Fifteen (15) ml of deionized water was added and thoroughly mixed using a magnetic stirrer for 20 minutes without heating so as to obtain a uniform solution. The solutions were then poured into a porcelain

crucible and placed in a furnace pre-heated at 500 °C for 15 minutes. When taken out of the furnace and cooled down, a white voluminous, highly-porous foamy substance was obtained and then grinded using a mortar and pestle to acquire the synthesized fine, white powders for CaB_2O_4. Following the combustion, the sample was calcined in a temperature of 900 °C for a fixed period of one hour in order to remove the unreacted organic residues and to enhance crystallinity of pure compound CaB_2O_4.

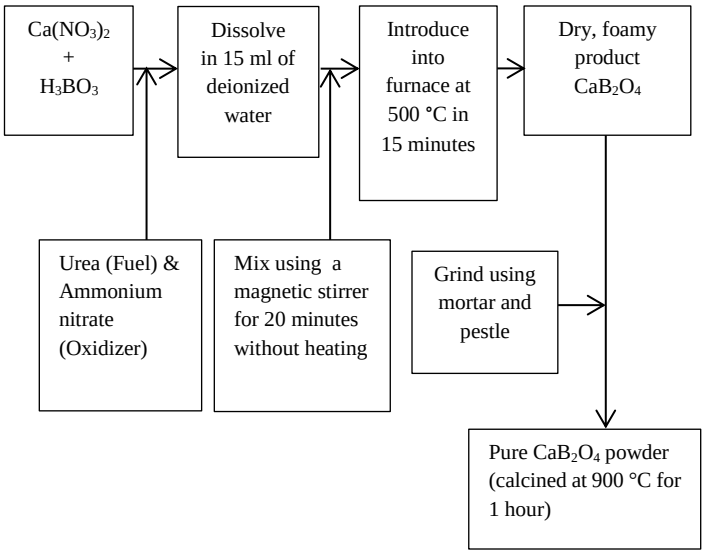

Fig. 1 Preparation of CaB_2O_4 powder by solution combustion method.

Characterization techniques

The prepared samples powder was characterized by X-ray diffraction (XRD) spectroscopy, field emission scanning electron microscopy (FESEM), and energy dispersive X-ray (EDX) analysis.

An XRD experiment was carried out at room temperature, 25°C, using a Siemens Diffractometer D5000 operating with CuKα radiation (λ = 1.5406 Å, 40 kV, 30 mA) in order to identify the crystal phase of the samples. The diffraction pattern was measured in steps 0.05° with 1s counting time per step, for 2-theta angle (2θ) ranging from 10° to 80°. The crystallite sizes of the CaB_2O_4 powder were calculated from the XRD peak intensity analysis using Debye-Scherrer formula (Langford and Wilson, 1978).

$$D = \frac{0.9\lambda}{\beta \cos\theta} \tag{1}$$

D is the crystalline size of the CaB_2O_4 powder in nm, λ is the radiation wavelength for CuKα radiation (λ = 1.5418 Å), θ is the diffraction peak angle and β is the broadening of the line (half width) measured at half its maximum intensity (in unit radians).

The morphology and elemental composition of the sample were determined using FESEM-EDX (ZEISS Supra 35VP, 15 kV). Weight fraction obtained from EDX analysis consequently led to determination of an effective atomic number (Z_{eff}) experimentally. Z_{eff} values were determined by using Eq. (2) and were compared with the theoretical results (Gonza´lez et al., 2007).

$$Z_{eff} = \sqrt[b]{(a_1 \times Z_1^b + a_2 \times Z_2^b + \ldots)} \tag{2}$$

with

$$a_i = \frac{n_i(Z_i)}{\sum_i n_i(Z_i)}, n_i = N_A Z_i \tag{3}$$

a_1, a_2,… are the fractional contents of the electrons belonging to different elements of atomic number Z_1 , Z_2 , … etc. in the composite; n_i is the number of electrons in one mole, belonging to each element Z_i and N_A is the Avogadro's number, 6.0221×10^{23} mol^{-1}. The value of b adopted for photon practical purposes is 2.94.

Percent error use in analysis between experimental and theoretical value can be obtained as follows:

$$Percent\,error\,(\%) = \frac{|Measured\,value - Actual\,value|}{Actual\,value} x\,100\% \tag{4}$$

Thermoluminescence measurements

Before irradiation of the CaB_2O_4 (calcining at 900°C) was performed, the virgin CaB_2O_4 powders were annealed at temperature 300 °C for one (1) hour using the TLD oven type LAB-01/400. After annealing, the sample powders were loaded into a small black plastic capsule. This capsule was made of opaque polyethylene capsules (IAEA type) of 3 mm diameter, 15 mm length and with 1 mm thick walls. Each capsule contains about 100 mg of TLD-powder. These capsules were then kept in the closed cabinet to avoid direct sunlight and ultraviolet radiation that may contribute to the development of a background signal. Fig. 2 displays the geometry set up for irradiating the capsule of CaB_2O_4 powder. Irradiation was performed by using Cobalt-60 (Co-60) source (GammaCell 220 Excel, MDS Nordion, Ottawa, Canada) with dose rate 1.3738 kGy h^{-1} on 9th January 2017. The set up for beam field size and standard source-surface distance (SSD) that were used was 10 x 10 cm^2 and 100 cm, respectively. After 24 hours irradiation, TL glow curves were measured and recorded using a Harshaw model 3500 TLD reader. Powder dispenser was used to aid in dispensing accurate amounts of dosimetric powders (15 mg) to the planchet of the 3500 reader. The process was performed with care to reduce any loss of powder during dispensing.

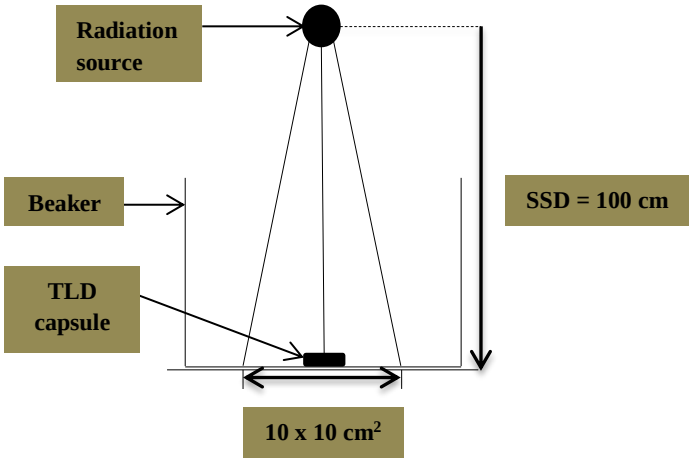

Fig. 2 Geometry set up for irradiating the capsule of CaB_2O_4 powder.

To record the dose response curve, the sample was irradiated to Co-60 at different gamma doses from 1 to 100 Gy at room temperature and the TL intensity was taken from the glow curve area. For comparison, glow curves were also recorded for standard, commercially available dosimeter LiF: Mg, Ti (TLD-100) powder. The total amount of electric current produced and area integral under the glow curves yields the TLD reading (or TL response) which signifies the radiation energy deposited and used for measuring the TL intensities.

The glow curve generated plots for the counts versus temperature automatically. Hence, the calculation formula in Eq. (5b) needs to be set in Excel in order to convert from counts to nanoamperes by using the time temperature profile (TTP) obtained from a previous study by Tengku Kamarul Bahri et al. (2017).

$$Q(nC)/t(s) = I(nA) \tag{5a}$$

This can also be written as

$$\frac{counts}{16000counts}(nC)\Big/\frac{t_{acq}(s)}{200\,glowcurve\,acquisition\,points}=I(nA) \quad (5b)$$

Q refers to the electrical charge converted from the light captured by the photomultiplier (PMT) that is collected from each sample in 16000 data points along. The t refers to the time when the dosimetric data is acquired in 200 channels and I is the electric current produced. The acquisition time in seconds (t_{acq}) can be found on the TTP that was created. In this study, the mean value of three readings was taken from each point to obtain a net TL signal and normalized to unit mass (g).

RESULTS AND DISCUSSION

Crystalline phase analysis

Fig. 3 shows the XRD patterns obtained for CaB_2O_4 powder, prepared by solution combustion method as-synthesized at 500 °C and calcined at 900 °C for 1 hour. The identified phases present in the patterns can be well-indexed to the reported CaB_2O_4 data in the Joint Committee on Powder Diffraction Standards (JCPDS) file no. 75-0640 with orthorhombic structure. However, as can be seen in Fig. 3, two minor phases at $2\theta = 24.33°$ and $25.92°$ (marked with asterisks) are observed in the CaB_2O_4 powder after calcining at 900 °C which corresponds to CaB_4O_7 phase. By comparing to XRD pattern as-synthesized, all the diffraction peaks become sharper thereby showing the amplified crystalline behavior of the heat-treated powders. It was reported that the high intensity of the diffraction peaks indicates good crystallinity of the particles (Liu et al., 2012).

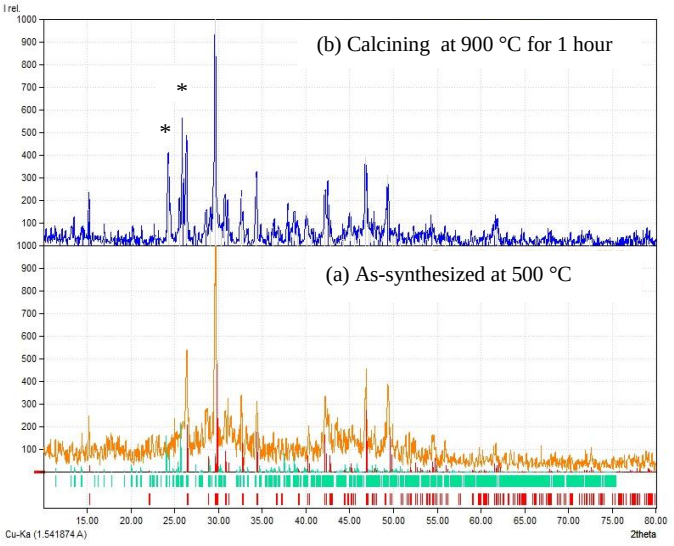

Fig. 3 XRD pattern obtained for the CaB_2O_4 powder, prepared by solution combustion method. (a) As-synthesized at 500 °C and (b) After calcining at 900 °C for 1 hour (red line is CaB_2O_4 phase and green line is CaB_4O_7 phase).

The crystallite sizes of the CaB_2O_4 powder have been calculated from the XRD peak intensity analysis using Debye-Scherrer formula in Eq. (1) and can be compared with the reported data (Shashkin et al., 1970). The size, together with percent error obtained on CaB_2O_4 powder, is indicated in Table 1. It was found that the crystallite size calculated for CaB_2O_4 is small in nanocrystal size (~27 nm) and is in good agreement with the standard value. As expected, crystallite size after calcination is smaller than as synthesized due to mechanism of product formation. When the calcium nitrate, together with boric acid, urea and ammonium nitrate with required stoichiometry is heated rapidly at 500 °C, it undergoes a melting and dehydration process. Later, it decomposes with frothing as a result of the formation $Ca/B(OH)(NO_3)_2$ in conjunction with other products like urea nitrate, biuret, HNCO and NH_3. This mixture then foams because of the generation of gaseous decomposition products as intermediates, leading to enormous swelling. The gaseous decomposition products are a mixture of nitrogen oxides, NH_3, and HNCO respectively. These gases are known to be hypergolic when coming into contact with each other. The foams break out with a flame due to the accumulation of the hypergolic mixture of gases. With an in situ temperature of 900 °C the whole foam further swells and burns to incandescence. At such high in situ temperatures, the foam decomposes to yield CaB_2O_4 (the high temperature foam) with low particle size thereby indicating the formation of stable product during calcination. This mechanism is proposed based on the reported literature for the preparation of α-Alumina particles (Patil et al., 2008).

Table 1 Crystallite size by XRD analysis with percent error of CaB_2O_4 powder.

Properties	Standard CaB_2O_4 powder (Shashkin et al., 1970)	CaB_2O_4 powder as-synthesized at 500 °C	CaB_2O_4 powder calcined at 900 °C
Crystallite size (nm)	27.4074	27.3941	27.3915
Percent error (%)	0.0000	0.0487	0.0579

Surface morphology analysis

A FESEM study was carried out to investigate the surface morphology of the nanocrystalline CaB_2O_4 particles. FESEM images of CaB_2O_4 as synthesized at 500 °C and calcined at 900°C are displayed in Fig. 4. The FESEM micrographs reveal that the morphology of the as-synthesized products was a non-spherical shape which formed a flake-like structure and changed into an irregular spherical structure when calcined at 900°C. This shows that the morphology of CaB_2O_4 nanocrystalline is influenced by the calcination temperature. It can be noticed from micrographs that all the particles are densely packed, thus preventing them from aging (Sheetal et al, 2013). The present results are also in good agreement with micrographs obtained by Vidyadhar (2013) which represents this image as having a nanocrystalline nature. Accordingly, crystallinity increases as the temperature increases. This may be attributed to the fact that the growth of the crystal takes place in different orientations. The crystallographic images clearly indicate that the particles are stacked on top of each other because of their mutual magnetic interactions (Vidyadhar, 2013).

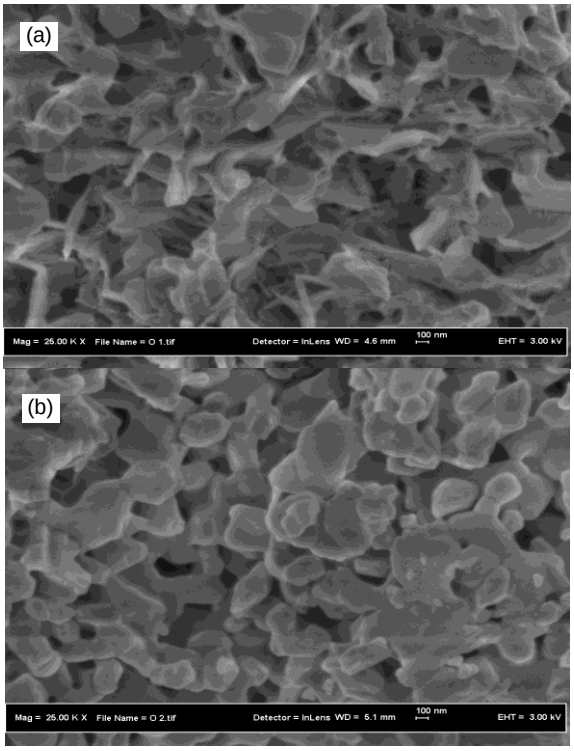

Fig. 4 FESEM images of nanocrystalline CaB_2O_4. (a) As-synthesized at 500 °C and (b) calcined at 900 °C for 1h.

Chemical analysis

Further information on the elemental composition of the samples can be provided by EDX analysis. Fig. 5 shows the EDX spectrum for one reading of CaB_2O_4 (which was calcined at 900 °C for 1h) while the weight fraction of each element in CaB_2O_4 is summarized in Table 2. The EDX results confirmed the presence of Ca, O and B elements in the crystals. The spectrum shows that CaB_2O_4 crystal powder consists of Ca, O and B elements. The corresponding result given in Table 2 shows that Ca, O and B weight fraction measured by EDX technique is in good agreement with the theoretical value, thereby revealing the effectiveness of the current preparation methods.

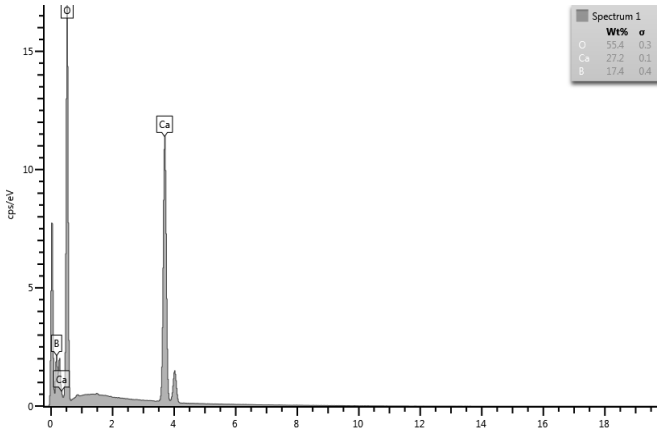

Fig. 5 EDX spectrum of CaB_2O_4 powder.

Table 2 Weight fraction of each element of CaB_2O_4 powder.

Component	Weight fraction (Theory)	Average weight fraction (Experiment)
O	0.5091	0.5272
Ca	0.3188	0.2724
B	0.1720	0.2005

By applying the result of the weight fraction to Eq. (2), the effective atomic number (Z_{eff}) can be obtained. The experimental and theoretical results for the Z_{eff} of CaB_2O_4 are tabulated in Table 3. The experimental Z_{eff} value is smaller than the theoretical value calculated. However, these experimental values still can be accepted because their percentage deviation is less than or equal to 10%. The experimental result showed that this material is equivalent to Z_{eff} of the bone, 13.2. This bone value is calculated from the weight fraction of the bone taken from ICRU Report 44 (ICRU, 1989). Bone is composed of the following main elements and weight percentage (wt %): hydrogen (H: 3.4 %); carbon (C: 15.5 %); nitrogen (N: 4.2 %); oxygen (O: 43.5 %); sodium (Na: 0.1 %); magnesium (Mg: 0.2 %); phosphorus (P: 10.3 %); sulfur (S: 0.3 %); and calcium (Ca: 22.5 %).

The absorbed dose in soft biological tissue exposed to ionizing radiation can be determined more accurately if the dosimetric material has a similar atomic composition of human tissue with effective atomic number of 7.42. In another study (Gowda et al, 2004), the radiation interactive characteristics of mixture or compounds that were similar to bone, soft tissue or any other body constituents can be identified for dosimetric purposes. For this reason, it justifies the use of CaB_2O_4 powder in radiation dosimetry.

Table 3 The experimental and theoretical values of effective atomic number for nanocrystalline CaB_2O_4 powder.

Material	Z_{eff} (average experimental)	Z_{eff} (theory)	Percent error (%)
CaB_2O_4	13.1	14.1	6.9
Bone, Cortical (ICRU, 1989)	-	13.2	6.8

Thermoluminescence analysis

TL glow curves are given in order to illustrate the changes in shape and peak temperature as a function of absorbed dose. It is believed that TL glow curves that show a maximum at middle range temperature of 140 °C to 200 °C have a low thermal fading, good reusability of samples and can avoid interference of TL with black body radiation (McKeever, 1993).

Fig. 6 shows TL glow curves for nanocrystalline CaB_2O_4 powder exposed to the irradiation dose in the range from 1 to 100 Gy of gamma ray of Co-60. The shape and the position of the TL peaks are almost constant in the dose range studied. All the curves consist of only one TL peak located at about 150 °C. This indicates that only one set of traps is being activated within the particular temperature range with its own value of activation energy (E) and frequency factor (s) (Puppalwar and Dhoble, 2012). TL intensity increases as the dose increases, without showing the saturation effect. This can be understood by the fact that, in the case of nanocystals, there still exist some particles that are not being targeted or not exposed to high energy radiation due to the very tiny size. Therefore, an increase of radiation dose to these nanoparticles leads to the addition of trapping centers and the luminescent centers. As a result, there is no saturation in nanocrystals even at higher doses.

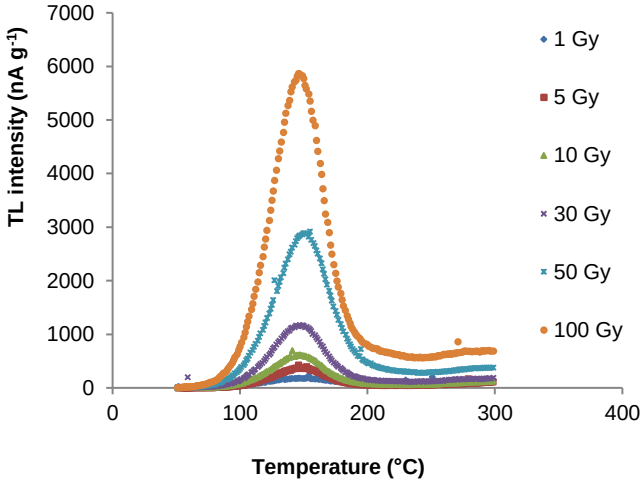

Fig. 6 TL glow curves of nanocrystalline CaB_2O_4 for different exposures gamma rays of Co-60.

The glow curves of TLD-100 powder are also given for comparison in Fig. 7. For TLD 100, the main peak is located at about 190 °C for low dose 1 Gy to 10 Gy. However, beyond 10 Gy, the TL intensity is seen to saturate at dose 30 Gy. There is one TL peak at dose 30 Gy and two TL peaks observed at dose 50 Gy and 100 Gy. All peaks are equally intense.

At dose 50 Gy of Co-60 gamma rays, two TL glow peaks of TLD-100 were observed at 224 °C and 179 °C; while at the higher dose 100 Gy, the TL peaks are located at 166 °C and 234 °C. As can be seen in Fig. 7, as the dose increases, the TL peak at 179 °C shifts to the lower temperature 166 °C and the TL peak at 224 °C shifts to a higher temperature 234 °C. This peak shift may be due to different kinds of traps produced by irradiation with different charge states occupying different energy levels (Haghiri et al., 2014). The incorporation of chemical impurities during sample preparation also caused the shift in the maxima of a TL glow peak temperature (Singh et al., 2011). The impurities are important in TL properties. It creates electron hole vacancies in the atomic structure of thermoluminescent crystals. The electron holes form traps within the atomic energy level structure. These result in the trapping of electrons ionized by radiation and are released when additional thermal energy is acquired to boost electrons out of the traps. The TL glow curve shows saturation at dose 30 Gy due to saturation of available trapping centers or luminescent centers responsible for the TL emission. Most of the electron traps have now been filled with electrons; electrons produced by additional given doses face a decreasing probability of finding an empty trap to lodge in (Glennie, 2003).

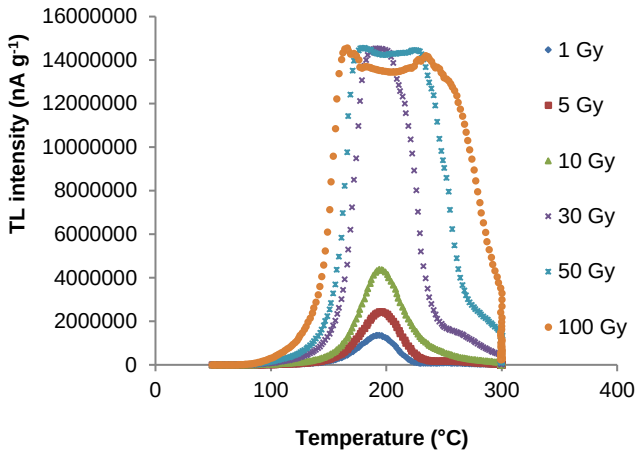

Fig. 7 TL glow curves of TLD-100 for different exposures gamma raysof Co-60.

An important property of a TL dosimeter material is that it exhibits a linear relation between TL intensity and absorbed dose. Many TL materials exhibit a nonlinear growth of TL intensity with absorbed dose over a certain dose region. The relationship between the TL intensity and gamma dose of nanocrystalline CaB_2O_4 and TLD-100 is shown in Fig. 8 and Fig. 9, respectively. The TL dose curve of CaB_2O_4 is observed to be linear in the studied dose range from 1 to 10 Gy at clinical dose levels with no saturation detected up to higher investigated dose 100 Gy. It can be noted that the stability of the TL glow curve leads to negligible changes in the integrated TL. The excellence of linearity response between dose and TL response to gamma radiation with high linear correlation, R^2= 0.9827 as compared to the TLD-100 powder with R^2= 0.9276 shows a remarkable result on the dosimetric feature of this material. Therefore, it could be expected that its application is not only suitable for clinical dosimetry, but also for high dose measurements in radiation dosimetry.

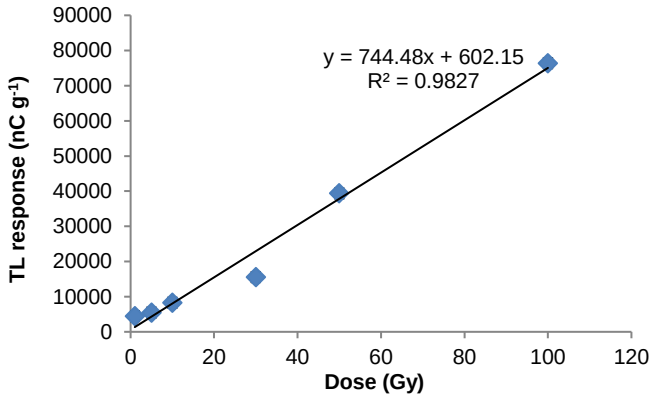

Fig. 8 TL response curve of nanocrystalline CaB_2O_4 exposed to different doses (1 to 100 Gy) of gamma rays of Co-60.

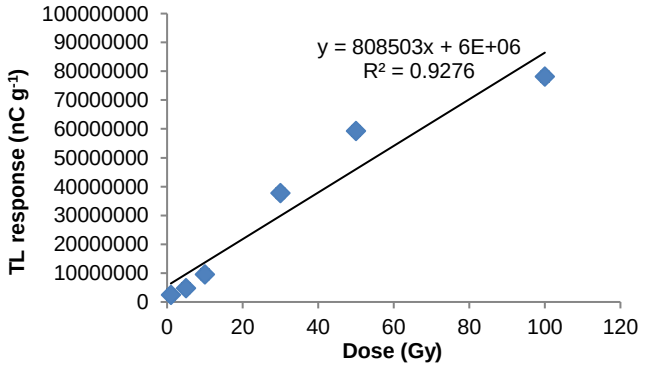

Fig. 9 TL response curve of TLD-100 exposed to different doses, 1 to 100 Gy of gamma rays of Co-60.

The average TL sensitivity and maximum TL glow curve peak temperature of nanocrystalline CaB_2O_4 and TLD-100 are summarized in Table 4. The TL sensitivity is defined as glow curve area (*TL*) per unit of mass of the dosimeter (*m*) and per unit of dose (*D*) of gamma rays (nC g^{-1} Gy^{-1}) as shown in Eq. (6). The data are given relative to the TL sensitivity of TLD-100 as in Eq. (7) (Chen and McKeever et al., 1997).

$$S(D) = \frac{TL}{m \cdot D} \tag{6}$$

$$R(D) = \frac{S(D)_{material}}{S(D)_{TLD-100}} \tag{7}$$

The TL sensitivity of nanocrystalline CaB_2O_4 and TLD-100 are expressed by $S(D)_{material}$ and $S(D)_{TLD-100}$, respectively. It has been found that the relative sensitivity of CaB_2O_4 has an average value of 0.001 over the dose range 1 Gy to 100 Gy. According to Soliman (2009), the average value of *R(D)* was 0.009 for a dose range from 1 Gy to 100 Gy. The results of such comparisons between the TL sensitivity of nanocrystalline CaB_2O_4 and TLD-100 are due to a photoelectric effect. The atomic cross section of the photoelectric effect is characterized by a strong dependence on the atomic number of the material and on photon energy. An increase in atomic number can cause the photoelectric effect to dominate over Compton effect which results in self absorption (Singh et al., 2007). It is known that TLD-100 is a low atomic number (*Z*) material having an effective atomic number, Z_{eff} =8.2; whereas CaB_2O_4 is a high *Z* material, Z_{eff} =14.1. It is believed that the TL peak of maximum temperature (T_m) in CaB_2O_4 at 150 °C is a well-defined, intense and reasonably stable peak, which is also supported by previous studies by Becker (1973). Therefore, it has a potential use as a thermoluminescence dosimeter.

Table 4 TL sensitivity and maximum TL glow curve peak temperature of nanocrystalline CaB_2O_4 and TLD-100.

Phosphor	Z_{eff}	T_m (°C)	Average $S(D)_{material}$ (nC g^{-1} Gy^{-1})	*R (D)*
CaB_2O_4	14.13	150	1410	0.001
TLD-100	8.20	190	1271413	1.000

CONCLUSION

CaB_2O_4 nanocrystals were successfully prepared by solution combustion method. The crystallite size of 27 nm was obtained and the XRD patterns exhibited the orthohombic structure. The FESEM micrograph revealed that the morphology of CaB_2O_4 nanocrystals was influenced by the calcination temperature. The as-synthesized result of 500 °C products was a nonspherical shape, which formed a flake-like structure and changed into an irregular spherical structure when calcined at 900 °C. The corresponding result showed that Ca, O and B weight fraction measured by EDX technique was in good agreement with the theoretical value, revealing the effectiveness of the current preparation methods. Also, the experimental result was concurrent with the theoretical value of effective atomic number CaB_2O_4, Z_{eff} = 14.1 (which was equivalent to the effective atomic number of the bone, Z_{eff} = 13.2 with error of 6.8 %). This material also exhibited striking TL properties useful for TLD. Glow curves showed a simple, well-defined and maximum temperature peak at around 150 °C. This was a reasonably stable peak and considered suitable for TLD. The TL response as a function of dose exhibited a linear dependence over the dose range 1 Gy to 100 Gy and high linear correlation R^2 = 0.9827 compared to the TLD-100 powder with R^2 = 0.9276. The significant dosimetric feature of these nanocrystals rendered it useful, not only in clinical dosimetry, but also in dosimeter of high irradiation dose measurements of gamma source. The largest application of high dose dosimetry is the sterilization of disposable, single-use medical

products. It is also used in food preparation to reduce pathogens and agricultural pest control.

ACKNOWLEDGEMENT

The authors would like to thank the Ministry of Education (MOE), Malaysia and Universiti Teknologi Malaysia for providing research grants and facilities. Our appreciation also goes to Mr. Ahmad Takim bin Saring from the School of Applied Physics, Faculty of Science and Technology, Universiti Kebangsaan Malaysia, 43600 UKM Bangi, Selangor Darul Ehsan, Malaysia for performing the Cobalt-60 irradiation procedure.

REFERENCES

Becker, K. (1973). *Solid state dosimetry*, CRC Press, Ohio.

Chen R. and McKeever S. W. S. (1997). *Theory of Thermoluminescence and Related Phenomena*, World Scientific, Singapore.

Fujimoto, Y., Yanagida, T., Koshimizu, M. and Asai, K. (2015). Photoluminescence, photo-stimulated luminescence and thermoluminescence properties of CaB_2O_4 crystals activated with Ce^{3+}, *Optical Materials*, vol. 41, pp. 49-52.

Glennie G. D. (2003), *A comparison of TLD: LiF:Mg,Ti and LiF:Mg,Cu,P, for measurement of radiation therapy doses*. Doctor of Philosophy, University of Virginia.

Gonza ´lez, P. R., Furetta, C., Calvo, B. E., Gaso, M. I. and Cruz-Zaragoza, E. (2007), Dosimetric characterization of a new preparation of $BaSO_4$ activated by Eu ions, *Nuclear Instruments and Methods in Physics Research B*, vol. 260, pp. 685-692.

Gowda, S., Krishnaveni, S., Yashoda, T., Umesh, T. K. and Gowda, R. (2004), Photon mass attenuation coefficients, effective atomic numbers and electron densities of some thermoluminescent dosimetric compounds, *PRAMANA-Journal of Physics*, vol. 63, pp. 529-541.

Haghiri, M. E., Saion, E., Soltani, N., Wan Abdullah, W. S., Navasery, M., Saraee, K. R. E. and Deyhimi, N. (2014), Thermoluminescent dosimetry properties of double doped calcium tetraborate (CaB_4O_7:Cu–Mn) nanophosphor exposed to gamma radiation, *Journal of Alloys and* Compounds, vol. 582, pp. 392-397.

White, D. R., Booz, J., Griffith, R. V., Spokas, J. J., and Wilson, I. J. (1989), Tissue substitutes in radiation dosimetry and measurement, *Journal of the International Commission on Radiation Units and Measurements*, vol. os23, pp. NP. (https://doi.org/10.1093/jicru/os23.1.Report44)

Langford, J. I. and Wilson, A. J. C. (1978), Scherrer after sixty years: a survey and some new results in the determination of crystallite size, *Journal of Applied. Crystallography*., vol. 11, pp. 102-113.

Liu, J., Zou, X., Xu, B., Luo, H., Lv, H., Hanab, L. and Yu, X. (2012), Y_2O_3:Eu^{3+} nanotubes self-assembled into flower aggregates, uniform nanotubes and monodisperse nanospheres: shape controlled synthesis and luminescent properties, *Crystal Engineering Communication*, vol. 14, pp. 3149-3155.

Mckeever, S. W. S. (1993), *Thermoluminescence of Solids*, Atomic Energy Press, China.

Patil, K. C., Hegde, M. S., Rattan, T. and Aruna, S. T. (2008), *Chemistry of nanocrystalline oxide materials: Combustion synthesis, properties and applications*, World Scientific, Singapore.

Puppalwar, S. P. and Dhoble, S. J. (2012), Determination of kinetic parameters of TL of Eu-doped $LiNaF_2$, *Indian Journal of Pure and Applied Physics*, vol. 50, pp. 855-858.

Santiago, M., Grasseli, C., Caselli, E., Lester, M., Lava, A. and Spano, F. (2001), Thermoluminescence of SrB_4O_7:Dy, *Physia. Status Solidi (A)*, vol. 185, no. 2, pp. 285-289.

Shashkin, D. N., Simonov, M. A. and Belov, N. V. (1970), Crystal structure of calciborite CaB_2O_4=$Ca_2[BO_3BO]_2$, *Doklady Akademii Nauk SSSR*, vol. 195, pp. 345-348.

Sheetal, S. P., Khatkar, Rajni Arora, V. B. T. and Mandeep (2013), Solution Combustion Synthesis and Structural Properties of YSrAl3O7: Tb Nanoparticles, *International Journal of Biotechnology and Bioengineering Research*, vol. 4, no. 4, pp. 291-298.

Singh, M. P., Sandhu, B. S. and Singh, B. (2007), Measurement of the effective atomic number of composite materials using Rayleigh to Compton scattering of 279 keV gamma rays, *Physica Scr*ipta, vol. 76, pp. 281–286.

Singh, S., Vij, A., Lochab, S., Kumar, R. and Singh, N. (2011), Thermoluminescence studies of BaS: Bi nanophosphors exposed to UV radiation, *Radiation Effects and Defects in Solids*, vol. 166, pp. 15-23.

Soliman, C. (2009), DyF_3: A promising new TL material for gamma dosimetry, *Nuclear Instruments and Methods in Physics Research* B, vol. 267, no. 14, pp. 2423-2426.

Tengku Kamarul Bahri, T. N. H., Hussin, R. and Ahmad, N. E. (2017), The influence of annealing temperature and heating rate on thermoluminescence properties of nanocrystalline calcium borate powder, *EPJ Web of Conferences*. vol. 156, pp.00010.

Vidyadhar , V. A., Sopan, M. R., Maheshkumar, L. M. and Kakasaheb, C. M. (2013), Influence of Zn^{2+} doping on the structural and surface morphological properties of nanocrystalline Ni-Cu spinel ferrite, *International Nano Letters*, vol. 3, pp. 29.

Wiedemann, E. and Schmidt, G. C. (1895), Über luminescenz, *Annals of Phy*sics, vol. 54, pp. 604-626.